Cavity-enhanced optical trapping of bacteria using a silicon photonic crystal

Thijs van Leest and Jacob Caro

Kavli Institute of Nanoscience Delft and

Department of Imaging Science and Technology

Quantitative Imaging Group

Delft University of Technology, Lorentzweg 1, 2628 CJ Delft, The Netherlands

Supporting Information

Fabrication

The photonic crystals are fabricated on silicon-on-insulator material with a 220 nm thick silicon device layer and a 2 µm thick buried oxide layer. In the designs the photonic crystal waveguides smoothly go over into ridge waveguides by gradually tapering down the adjacent photonic crystal on either side. The lithographic patterns are e-beam written in a 120 nm thick ZEP-520A resist. The patterns are transferred to the silicon by reactive ion etching in an SF_6/O_2 plasma at a substrate temperature of -120 °C. SEM pictures of the cavities are shown in Figure S1a-c.

A fluidic channel is created on the photonic crystals using a dry film resist technique. The channel is made in the first dry film layer[1] (TMMF S2030, 30 µm thick), laminated onto the chip, using deep UV lithography. The channel is 50 µm wide and is aligned orthogonal to the waveguides, with the photonic crystals in the centre (see Figure S1d). Then, the photonic crystals are underetched in an HF solution, to form membranes. These yield cavities with a higher Q factor as a result of symmetric cladding and allow easy infiltration of the etched holes with water. To seal the channel, a second TMMF layer is laminated on the first one.

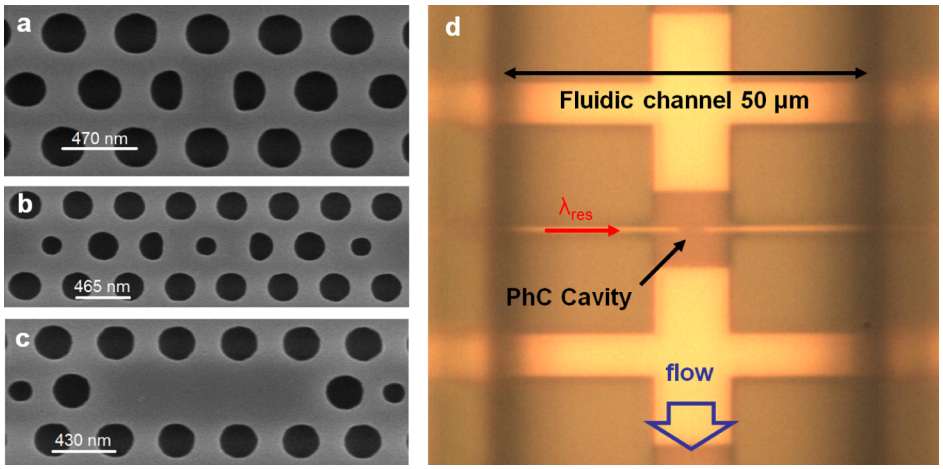

FIGURE S1. (a-c) SEM pictures of the fabricated H0, H1 and L3 cavities, respectively, with scale bars equal to the lattice constants. (d) microscope picture of a photonic crystal centred in the fluidic channel.

Measurement set-up

For the optical measurements the chip can be placed in a holder with O-ring seals, enabling control of the flow using millimetre thick tubing and a syringe pump. An alternative way to create a steady flow is to put small droplets of medium with bacteria on the entrance and exit ports of the channel. The experiments are performed in an end-fire set-up, using a lensed PM-fiber to couple light into the waveguide. A tunable infrared laser (Santec TSL-210) is used as source, in combination with an amplifier (Amonics AEDFA). Top view observations are performed with an Ultrazoom Navitar microscope system using an ELWD 50X/0.55 Olympus objective and a Genie HC-640 Dalsa as the recording camera.

Estimate of the input power and the modal energy

The input power presented to a cavity by the photonic crystal waveguide is estimated from the measured transmitted power at the resonance frequency of the cavity. From coupled mode theory[2] one can derive that, for a given value of $Q_\perp$, the energy stored in the cavity reaches a maximum for $Q_\parallel = Q_\perp$, corresponding to a transmission of 25%. Derivation of this result starts from Eq. (18) on p. 208 of Ref. *(2)*, which applies to a waveguide/cavity/waveguide system including radiation losses, rewritten for our purpose:

$$\frac{dA}{dt} = -i\omega_{\mathrm{res}}A - \frac{A}{\tau_\parallel} - \frac{A}{\tau_\perp} + \sqrt{\frac{1}{\tau_\parallel}}S_1^+ \qquad (1)$$

Here A is the time-dependent field amplitude of the cavity mode, normalized such that $|A|^2$ is the energy of the mode. ω_{res} is the resonance frequency, $\tau_\parallel = 2Q_\parallel/\omega_{\mathrm{res}}$ is the in-plane resonance lifetime (including the *two* identically coupled waveguides), $\tau_\perp = 2Q_\perp/\omega_{\mathrm{res}}$ is the out-of-plane resonance lifetime (representing radiation losses) and S_1^+ is the field amplitude of the waveguide mode going towards the cavity (such that $|S_1^+|^2$ is the power of the mode going towards the cavity) For operation at the resonance frequency ($A \sim e^{-i\omega_{\mathrm{res}}t}; \frac{dA}{dt} = -i\omega_{\mathrm{res}}A$) we find for the modal energy of the cavity

$$|A|^2 = \frac{\tau_\parallel {\tau_\perp}^2}{(\tau_\parallel+\tau_\perp)^2}|S_1^+|^2 = \frac{2Q_\parallel {Q_\perp}^2}{(Q_\parallel+Q_\perp)^2}\frac{|S_1^+|^2}{\omega_{\mathrm{res}}} = 2T(\omega_{res})Q_\parallel\frac{|S_1^+|^2}{\omega_{\mathrm{res}}}, \qquad (2)$$

where the fraction in front of $|S_1^+|^2/\omega_{\mathrm{res}}$ is an energy enhancement factor. For a given $Q_\perp$, this fraction and thus the modal energy is maximum for $Q_\parallel = Q_\perp$. From $T(\omega_{\mathrm{res}}) = [Q_\perp/(Q_\parallel + Q_\perp)]^2$, the expression of the transmitted power at resonance, it then follows $T(\omega_{res}) = 25\%$.

In principle, we thus can make a quick estimate of the power presented to a cavity by measuring its in-plane output power at the resonance frequency. In practice, however, we have to include further considerations. One assumption made in the design process[3] is that coupling of the waveguides to the cavity does not affect $Q_\perp$. However, in a further iteration of the design simulations we find that $Q_\perp$ has become somewhat smaller as a result of introduction of the coupling, so that $T(\omega_{\mathrm{res}})$ is smaller as well. When the fabricated geometries of the cavities are also taken into account in the simulations, we find $T(\omega_{res}) =$

17%, 13% and 10% for the H0, H1 and L3 cavities, respectively. These numbers are the basis of the power estimates in Table 1 of the manuscript.

Using the above theoretical value of 25% for the transmission at resonance, the modal energy is given by $|A|^2 = (Q_{||}/2)|S_1^+|^2/\omega_{\mathrm{res}}$, which is the expression used in the introduction section of the article (where E_{cav}=$|A|^2$and $P_{\mathrm{in}} = |S_1^+|^2$). Inserting $Q_{||} = 4600$ (based on $Q_{\parallel} = Q_{\perp} = 2Q_{\mathrm{tot}} = 4600$; see above), and taking into account that the evanescent field decays exponentially with the distance from the surface, so that the fraction of the modal energy seen by a bacterium amounts to[3] ≈3.5%, it follows that the estimated energy available for excitation of the Raman effect in a trapped bacterium equals $12.8\times|S_1^+|^2/f_{\mathrm{res}} = 12.8\times|S_1^+|^2\lambda_{\mathrm{res}}/c$. On the other hand, since in conventional Raman laser tweezers the energy is typically focused on the length scale of the wavelength, one has $E_{focus} = P_{\mathrm{laser}}\lambda_{\mathrm{laser}}/c$. Therefore, we arrive at a factor on the order of ten for the enhancement of the Raman effect with a photonic crystal cavity as compared to Raman laser tweezers.

Bacteria culturing

The vegetative *B. subtilis* and *E. coli* bacteria are cultured in a peptone growth medium overnight and used in trapping experiments within one day. The medium with bacteria is applied to the microfluidic channel without dilution (~10^8 bacteria/ml) and has a salt concentration of about 85 mmol/l. The solutions of *B. subtilis* spores are prepared by scraping the spores from a starved culture on an agar plate and adding the scrapings to demi-water. NaCl is added to obtain a concentration of 25 mmol/l, in order to have a predictable cavity-spore surface separation in the measurements.

Pre-processing of frames for position tracking

The confined Brownian motion of a spore in the trap is determined from video observations made with bright field illumination, without fluorescent labelling of the spores. The frames of a video, obtained with an integration time of 3 ms and a frame rate of 300 fps, are pre-processed before applying the tracking software. The pre-processing involves cropping to the region of interest and subtraction of the background image, which is an averaged reference frame without spore (result in Figure S2a). Then a Gaussian filter is applied to suppress noise (result in Figure S2b) and finally the area of the spore is determined (Figure S2c). Further, in tracking the position of a spore, vibrations of the microscope body with respect to the chip are removed by comparing for each frame the position of the chip to its position in the reference frame and by correcting for possible deviations. As the intensity distribution of the light reflected by the spore does not always have the symmetry of the illuminated part of the spore and may fluctuate in time, we use the contour of the spore to determine its centre in the *x*-*y* plane (by summing the position vectors of the pixels completely or partly inside the contour). A spore spans 15-20 pixels of size 64×64 nm^2 in any direction. It is found that the accuracy in the localization of the centre is on the order of 3 nm. For low excitation powers the spore tends to rotate in the trap, while the rotation axis may not pass through the centre. In that case the localization is less accurate.

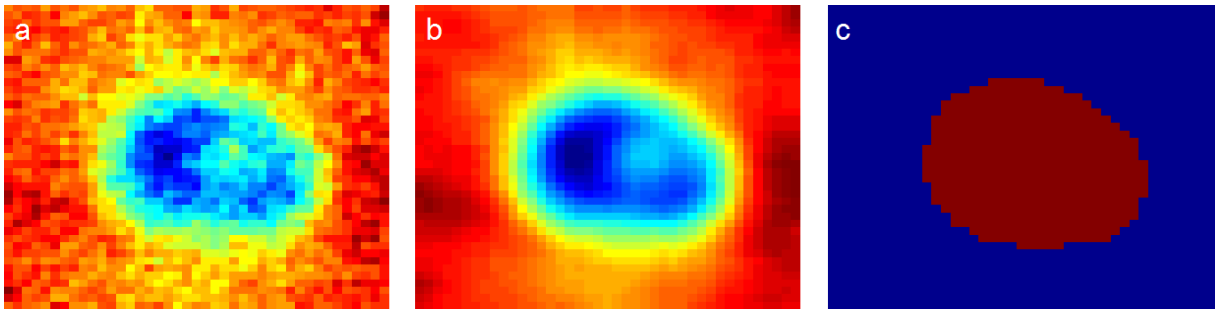

FIGURE S2. Frames after successive pre-processing steps. (a) region of interest after cropping and background subtraction, showing a spore, (b) the same frame after application of a Gaussian filter, (c) uniform intensity distribution of the spore and its environment, defining the spore's area for the determination of its centre.

Motion blur correction function

In deriving the trap stiffness of the cavities from the Brownian motion of a trapped spore, the motion blur correction function[4] $S(\alpha)$ is applied to correct for the motion blur induced by the exposure time of the camera:

$$S(\alpha) = \frac{2}{\alpha} - \frac{2}{\alpha^2}(1 - e^{-\alpha}), \quad \text{with} \quad \alpha = \frac{W}{\gamma/k} \tag{3}$$

Here W is the camera exposure time, γ the friction factor and k the trap stiffness. The friction factor is given by Faxen's law[5] for a particle near a surface:

$$\gamma = \frac{6\pi R\eta}{1 - \frac{9}{16}\left(\frac{R}{h}\right) + \frac{1}{8}\left(\frac{R}{h}\right)^3 - \frac{45}{256}\left(\frac{R}{h}\right)^4 - \frac{1}{16}\left(\frac{R}{h}\right)^5} \tag{4}$$

Here R is the radius of the particle, h the distance between particle and surface and η the viscosity of the fluid.

Trapping stiffness calculations

The calculated trapping forces are determined by integrating the stress tensor over a cube enclosing the spore model.[6] The integral involves large numbers that to a large extent cancel out to result in small net forces. The numerical errors accumulated can give large contributions, especially in non-symmetric field distributions such as the evanescent field. Extra effort is therefore made in the simulations to optimize the settings for meshing, considering the trade-off between calculation time and numerical errors in the calculated force. As the mode-field pattern decays exponentially away from the surface of the cavity, the numerical error contribution to the total force decreases as well. It therefore suffices to use a fine mesh, with dimensions down to 2 nm, only at the bottom part of the integration cube and around the cavity itself.

For each calculated force acting on a spore, we also calculate the force for the same simulation settings without the particle in the cube. For the Maxwell stress tensor method the total force should then be zero. Any net contribution remaining is therefore used as the main

source of error in the actual calculation for the spore. We require this error to be less than 25% of the force. By subtracting the error from the actual force result, the net result will be much more accurate. An example of this procedure is presented in Figure S3. The forces presented in Figure 5 were obtained according to this procedure.

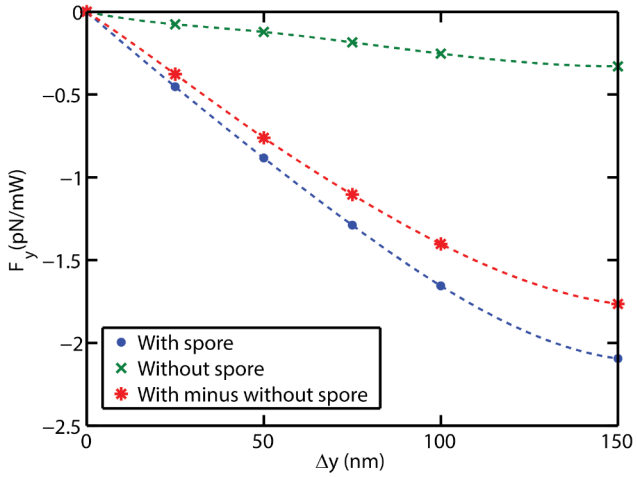

FIGURE S3. Force calculations for the H0 cavity, as a function of displacement of the spore in the y-direction (a). Calculated including (blue dot) and excluding (green cross) the spore inside the force calculation box and the net result (red asterisk).

References

(1) Wangler, N.; Gutzweiler, L.; Kalkandjiev, K.; Muller, C.; Mayenfels, F.; Reinecke, H.; Zengerle, R.; Paust, N. *J. Micromech. Microeng.* **2011**, *21*, 0960-1317.

(2) Joannopoulos, J.D.; Johnson, S.G.; Winn, J.N.; Meade, R.D. *Photonic Crystals: Molding the flow of light*; Second Edition, Princeton University Press, Princeton, 2008, pp 208-210.

(3) van Leest, T.; Heldens, J. ; van der Gaag, B.; Caro, J. "Photonic crystal cavities for resonant evanescent field trapping of single bacteria." In *Biophotonics: Photonic Solutions for Better Health Care III*, Proceedings of SPIE 8427, Brussels, April 16-19, 2012.

(4) Wong, W.; Halvorsen, K. *Opt. Express* **2006**, *14*, 12517-12531.

(5) Schäffer, E.; Nørrelyke, S.F.;Howard, J. *Langmuir* **2007**, *23*, 3654-3665.

(6) Lumerical Solutions, Inc. http://www.lumerical.com/tcad-products/fdtd/